Charm Production in CC DIS at HERA

Jae D. Nam
Temple Univ.

Motivations

- Charm cross section measurement in high-Q^2 charged current (CC) DIS.

  $\rightarrow$ Constraints on $s(x, Q^2)$

- Previous measurements on strangeness of the proton.

  $\rightarrow$ CCFR/NuTeV : $\frac{\int_0^1 dx[xs+x\bar{s}]}{\int_0^1 dx[x\bar{u}+x\bar{d}]} \sim 0.5$ at $x \sim 0.1$, $\quad Q^2 \sim 10\ GeV^2$

  $\rightarrow$ ATLAS : $\frac{s+\bar{s}}{\bar{u}+\bar{d}} \sim 1.0$ at $x = 0.023, Q^2 = 1.9\ GeV^2$

- Improved determination of strange sea quark content in the proton (right)
  - Charm production in neutrino-nucleon scattering by CCFR/NuTeV, NOMAD, CHORUS
  - $W + c$ production by CMS and ATLAS

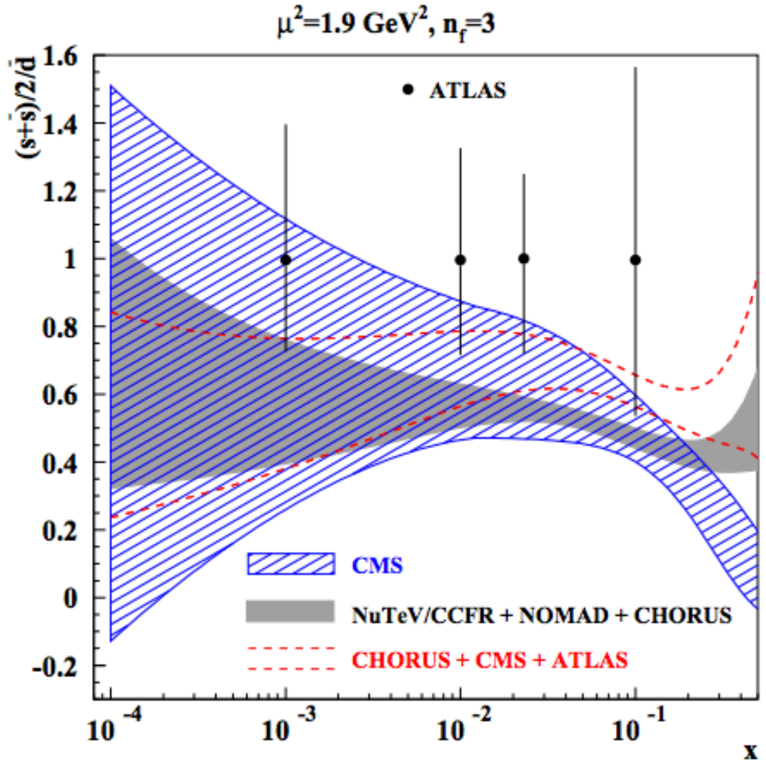

FIG. V.1: The 1σ band for the strange sea suppression factor $r_s = (s + \bar{s})/2/\bar{d}$ as a function of the Bjorken x obtained in the variants of present analysis based on the combination of the data by NuTeV/CCFR [2], CHORUS [4], and NOMAD [3] (shaded area) and CHORUS [4], CMS [10], and ATLAS [11] (dashed lines), in comparison with the results obtained by the CMS analysis [10] (hatched area) and by the ATLAS *epWZ*-fit [9, 11] at different values of x (full circles). All quantities refer to the factorization scale $\mu^2 = 1.9$ GeV^2.

Charm production in CCDIS at HERA

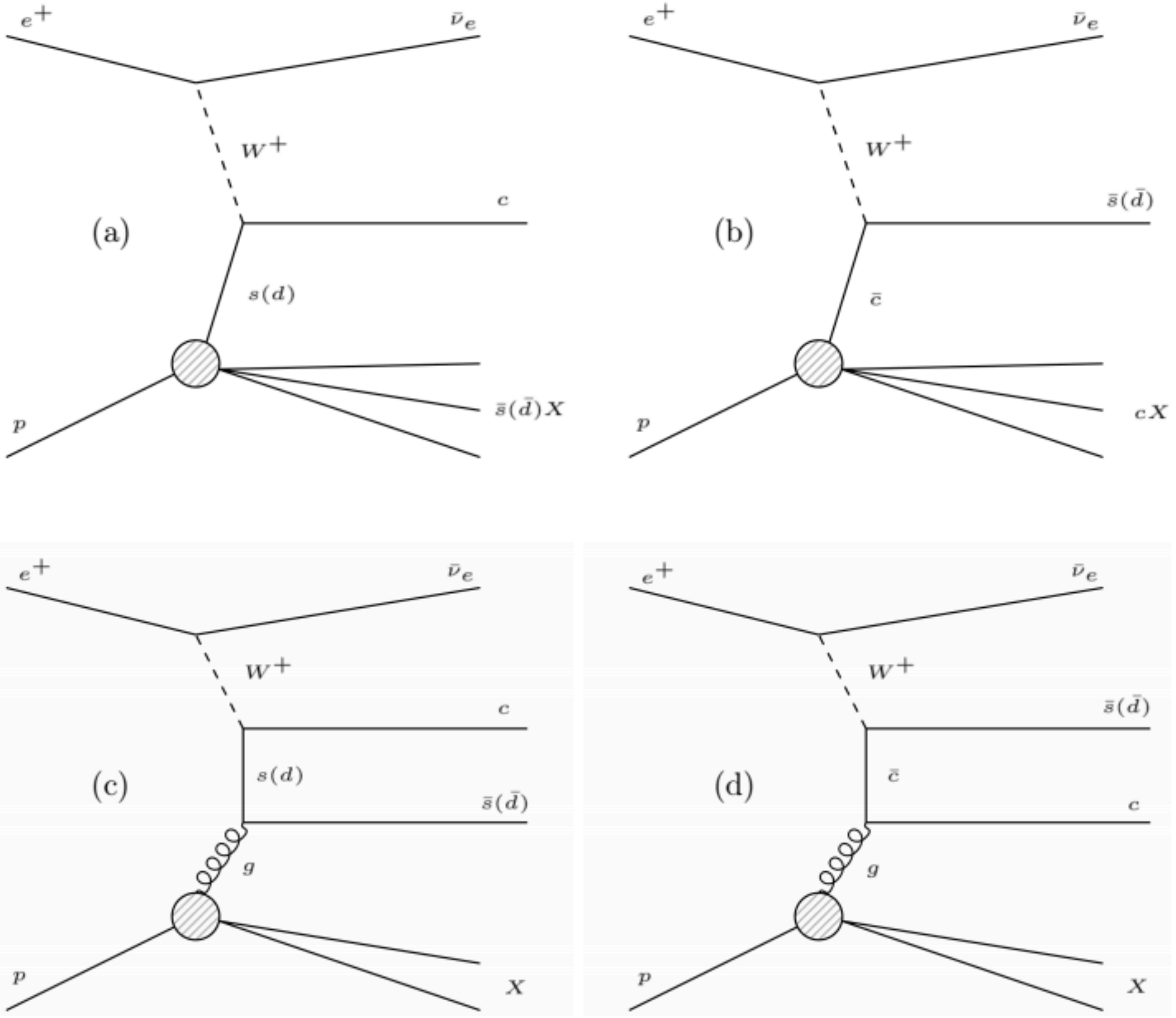

- QPM-like processes (a, b)
  - Small active charm content in the proton.
    → small contribution of (b)
  - Cabibbo-suppressed $d \rightarrow c$ transition.
  - Sensitive to the strangeness in the proton.
- BGF-like processes (c, d)
  - Sensitive to the gluon content in the proton.
- Model-dependent strange quark content extraction.
- Final state gluon splitting (below).

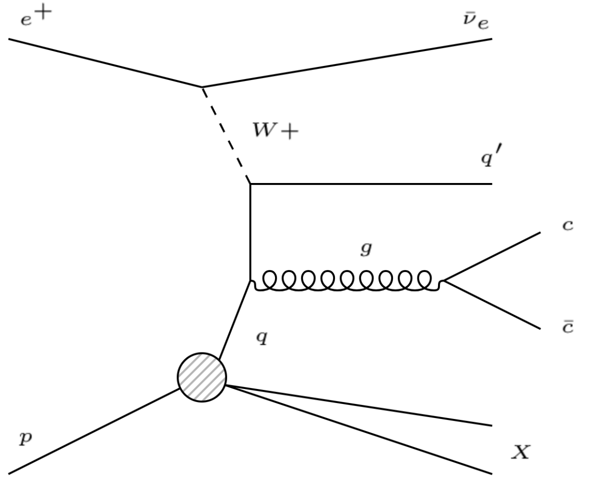

DATA & MC & Kinematic variables

Data

- HERA II ($L \cong 360\, pb^{-1}$)
  - $e^{-}p$: $05e, 06e$ w/ $L \cong 185\, pb^{-1}$
  - $e^{+}p$: $0304p, 0607p$ w/ $L \cong 173\, pb^{-1}$

Year	Collision	Integrated Luminosity (pb^{-1})
2003/04	$e^{+}p$	~ 38
2004/05	$e^{-}p$	~ 133
2006	$e^{-}p$	~ 52
2006/07	$e^{+}p$	~ 135

- Kinematic variables (x, y, Q^2) defined by using Jacquet-Blondel Method.

$$y_{JB} = \frac{\sum_h (E - p_z)_h}{2E_{e,beam}} \qquad Q^2_{JB} = \frac{p^2_{T,h}}{1 - y_{JB}} \qquad x_{JB} = \frac{Q^2_{JB}}{s y_{JB}}$$

MC

- DIS
  - Inclusive CCDIS MC, DJANGOH 1.6, ARIADNE 4.12, CTEQ-5D.
- Background
  - Inclusive NCDIS MC: DJANGOH 1.6, ARIADNE 4.12, CTEQ-5D
  - Photoproduction MC: HERWIG, resolved & direct
  - Background contribution was found to be negligible.
- The kinematic variables (x, y, Q^2) obtained from the lepton information.

$$Q^2 = -(k - k')^2 \qquad x = \frac{Q^2}{2pq} \qquad y = \frac{pq}{pk}$$

DIS Selection Summary

General Selection	
Trigger	FLT 60 || 63 || 39 || 40 || 41 || 43 || 44 SLT EXO 4 TLT EXO 2 || EXO 6 DST 34
DQ	EVTAKE, POLTAKE, MVDTAKE, STTTAKE
p_T	p_T > 12 GeV p'_T > 10 GeV
Kinematic	200 < Q2 < 60,000 GeV2 y < 0.9

Tracking Based Selection	
Vertex	|Zvtx| < 30 cm
ϕcal - ϕtrk	dϕ < 90 degrees
Beam Gas Trk	Ntrkvtx > 0.125 * (Ntrk - 20)

**Based on 0607p CC MC by Ciesielski & Oliver

Calorimeter Based Selection	
Timing	Consistent with ep interaction
PhP, Beam Gas	Vap/Vp < 0.25 if (Pt < 20 GeV) Vap/Vp < 0.35 else
Cosmics	Reject if: Ncell < 40 or (BAC/BRMU cosmic muon) or E_RCAL > 2 GeV and f_RHAC > 0.5 or E_BCAL > 2 GeV and f_BHAC > 0.85 or f_BHAC1 > 0.7 or f_BHAC2 > 0.4 or E_FCAL > 2 GeV and f_FHAC < 0.10 or f_FHAC > 0.85 or f_FHAC1 > 0.7 or f_FHAC2 > -.6
Halo Muon	Reject if: MaxEtCell_nr <= 16384 and RCAL asosE > 0.3 GeV (FCAL) or Tsu_halo > 0 (TSUBAME in BCAL) or (BAC/BRMU halo muon)
NC DIS	Reject if: PT < 30 GeV&& E-Pz > 30 GeV && E_e > 4 GeV && E_in < 5 GeV && (Ptrk/Ee > 0.25 for 15 < θe < 164 or Ete > 2 GeV for θe > 164)

yellow – Varies between run periods
-STTTAKE = 0 for 05e data
-FLT 63 active after run 54115

green – Only applied on data
-Timing cut only on data

Control plots – event

e^+p

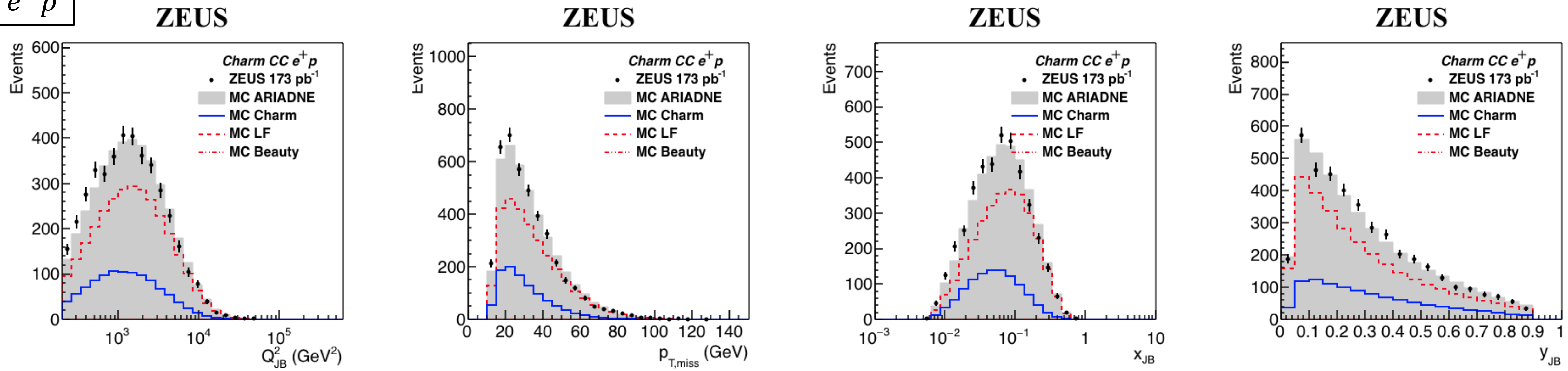

e^-p

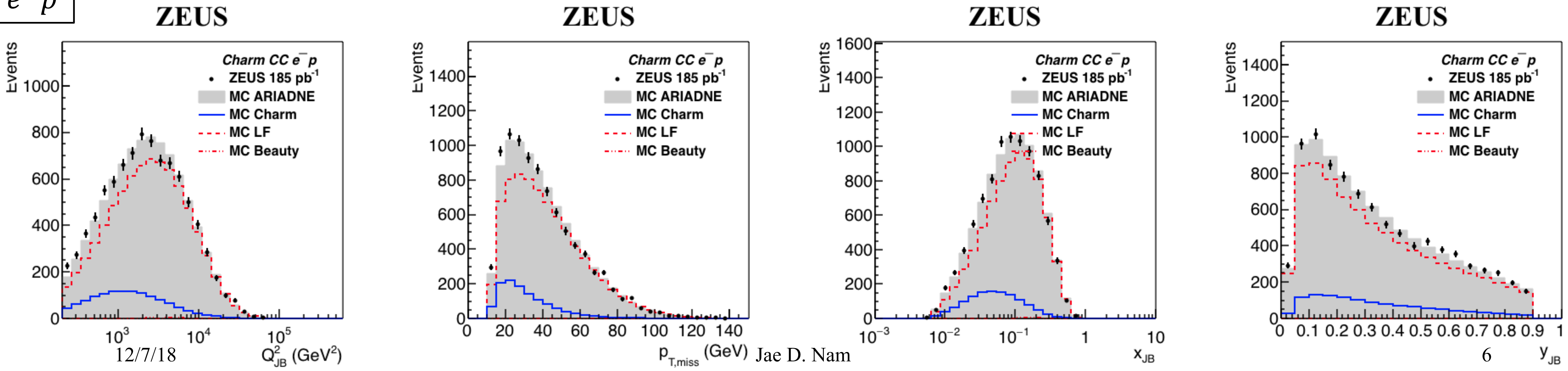

Charm Identification

Lifetime-tagging Method

- 2D decay length (L_{xy}) projected onto Jet axis.
  - LF → Short-lived, Symmetric decay length.
  - Charm → Long-lived, Asymmetric.

- LF contribution (background) suppressed by mirroring decay length distribution about $L_{xy} = 0$.

$$(N_{L+} - N_{L-}\,, N_{S+} - N_{S-})$$

*S = significance

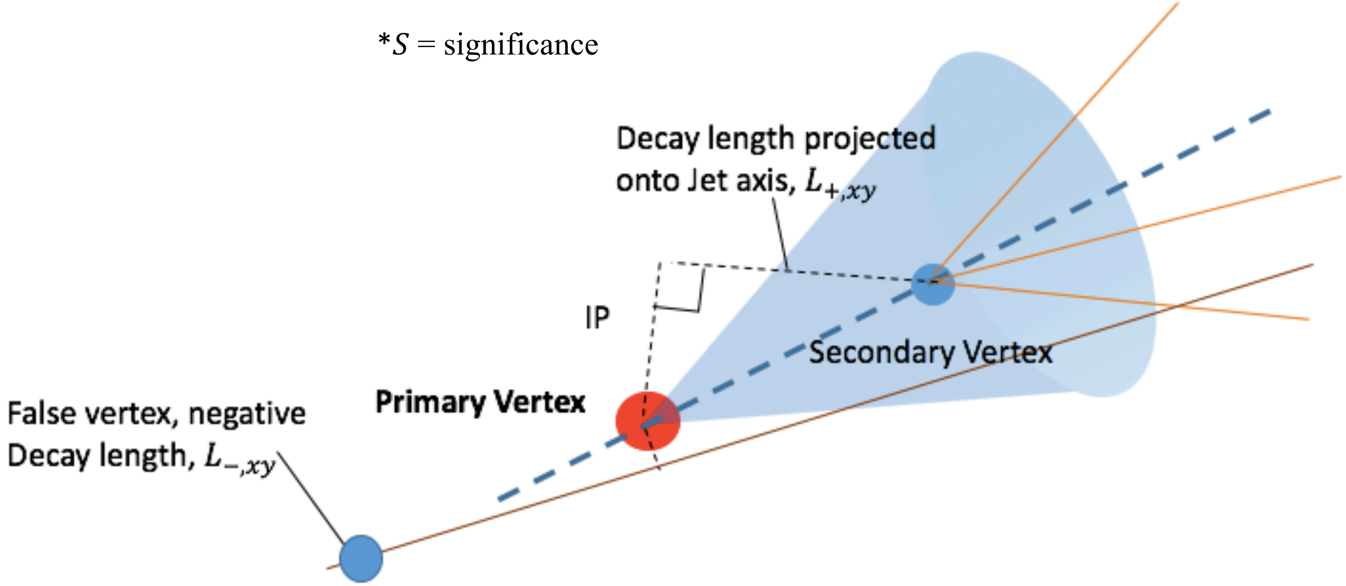

Jet Selection	Reconstructed by using kT algorithm in the massive mode.
	$E_T^{jet} > 5\ GeV$
	$-2.5 < \eta^{jet} < 2.0\ (1.5\ for\ 05e)$
SecVtx Selection	$\chi^2/N_{dof} < 6$
	$\lvert Z_{secvtx} \rvert < 30\ cm$
	Distance to beam spot $\sqrt{\Delta x^2 + \Delta y^2} < 1\ cm$
	$M_{secvtx} < 6\ GeV$
	$N_{secvtx}^{trk} > 2$

- E_T^{jet} and η^{jet} cuts further define the kinematic phase space of the measurement.

Control plots – jet & secondary vertex

e^+p

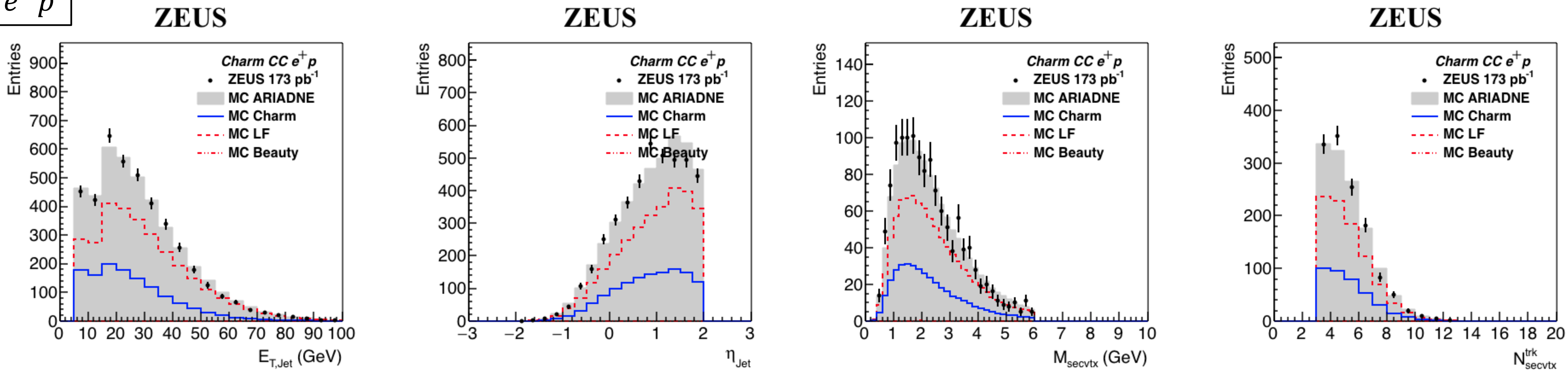

e^-p

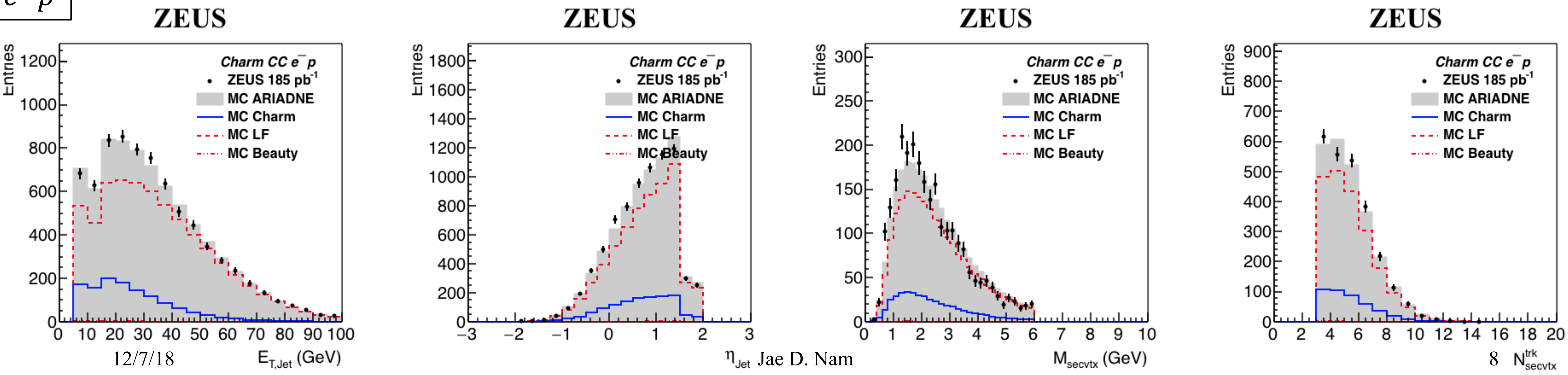

Decay Length Plots

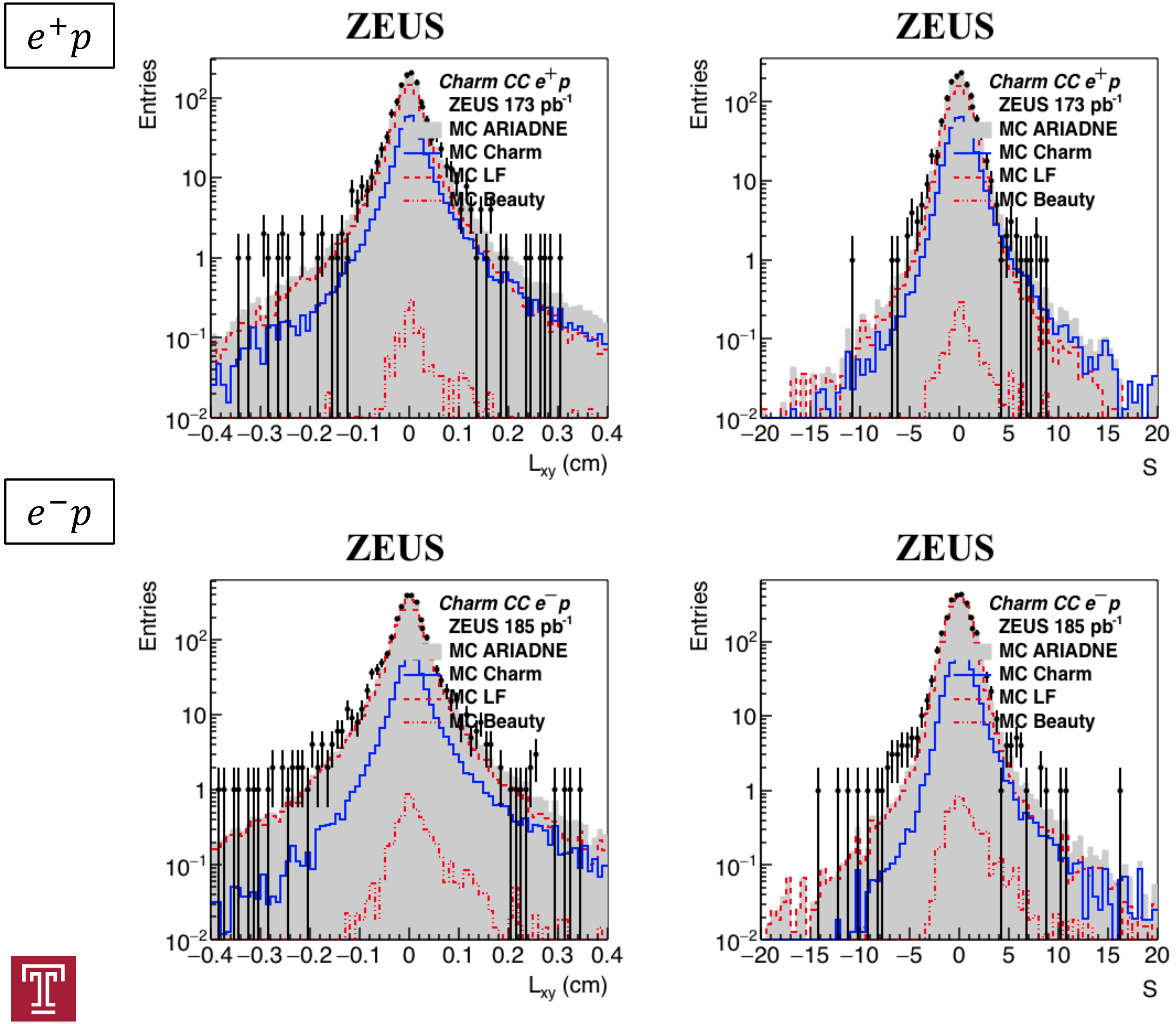

- Asymmetric charm signal observed.

- The high symmetry and large statistics around $S \sim 0$ contributes to a large statistical uncertainty in the low bin regions in $|S|$.

- A significance threshold cut $|S| > 2$ was applied to reduce overall statistical uncertainty.

Mirrored Decay Length

e^+p

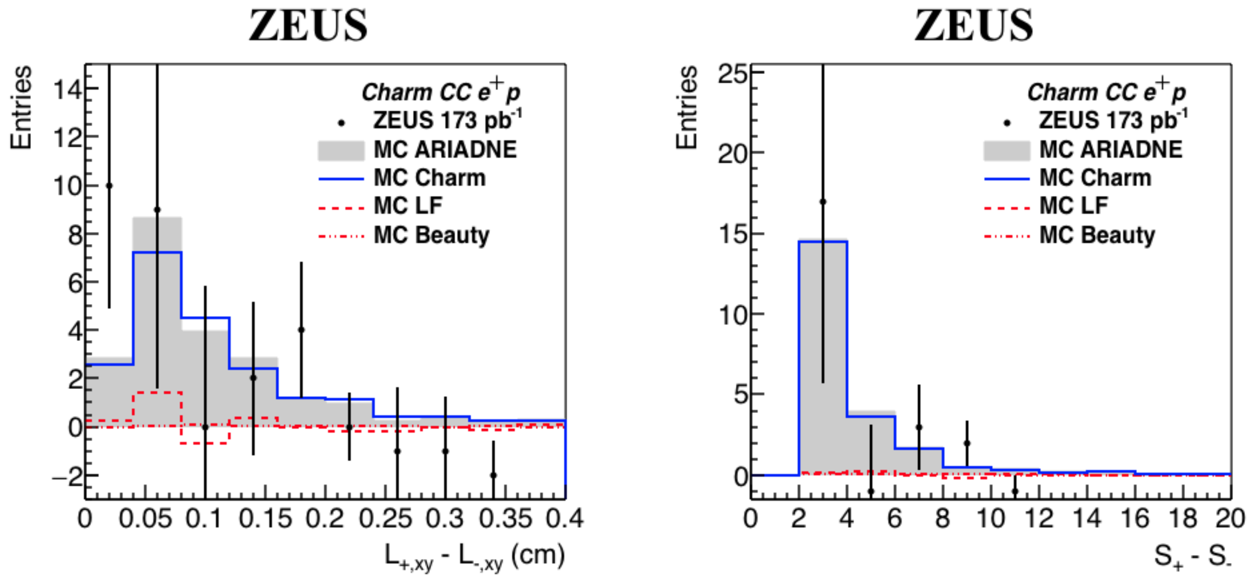

e^-p

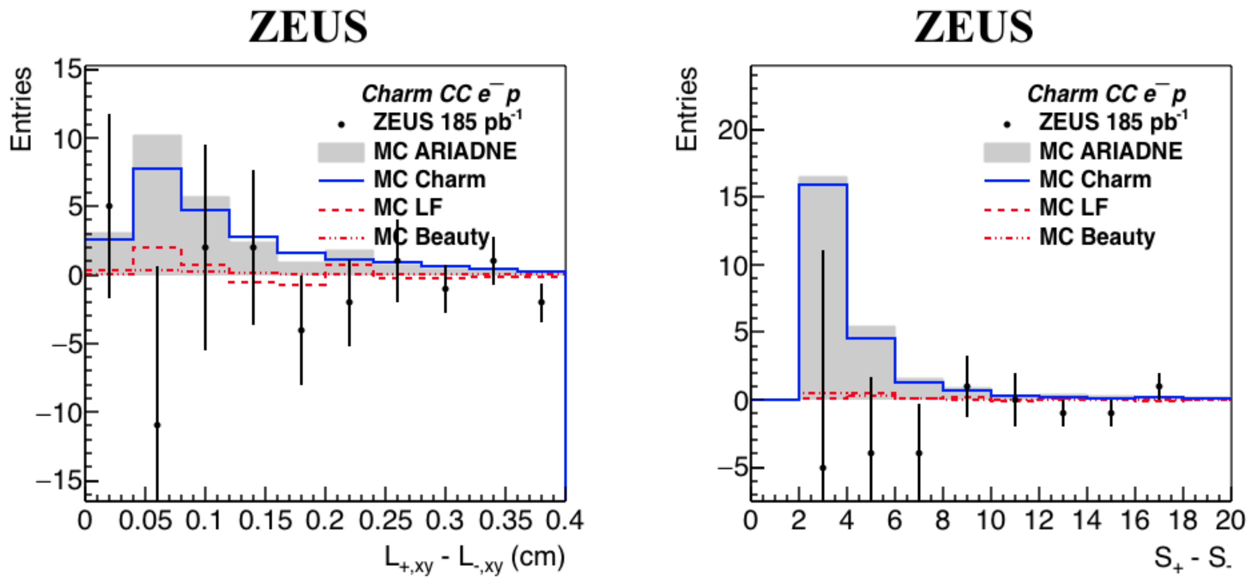

- Significance cut applied at $|S| > 2$.
- Charm signal observed with LF contribution (Background) suppressed.
- Surviving events are split into 2 bins in Q^2 to unfold charm production cross section, $\sigma_{charm,CC}$.

Charm signal & Charm generated

e^+p

M_{signal}

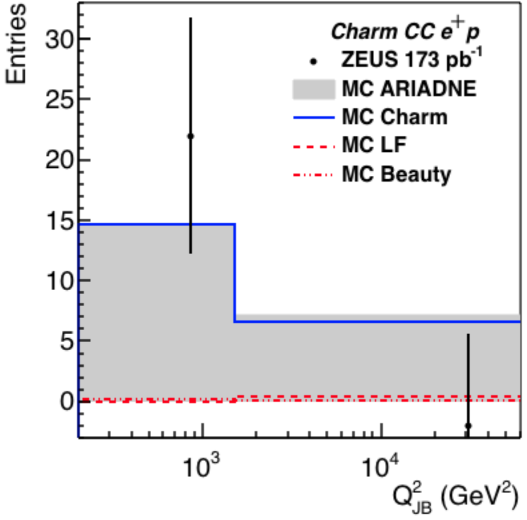

N_{kin}

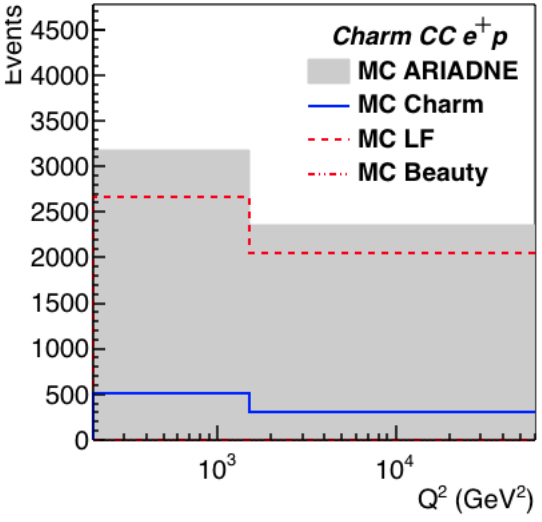

N_{gen}

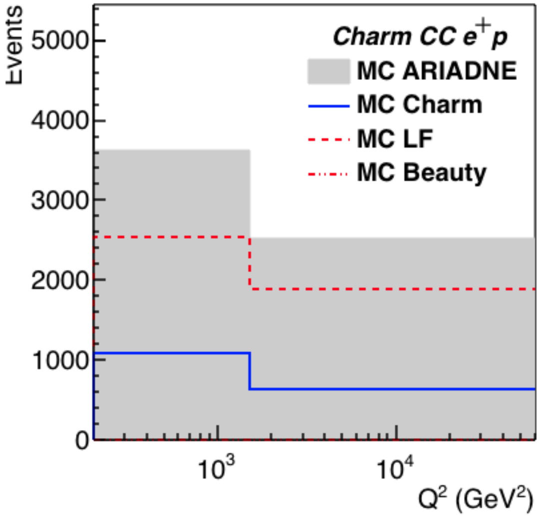

- Surviving events after the background subtraction are split into two bins in Q^2 $(200-1500\ GeV^2,\ 1500-60000\ GeV^2)$.

e^-p

M_{signal}

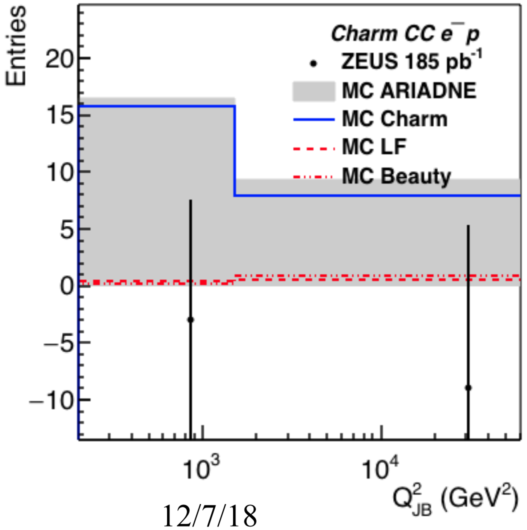

N_{kin}

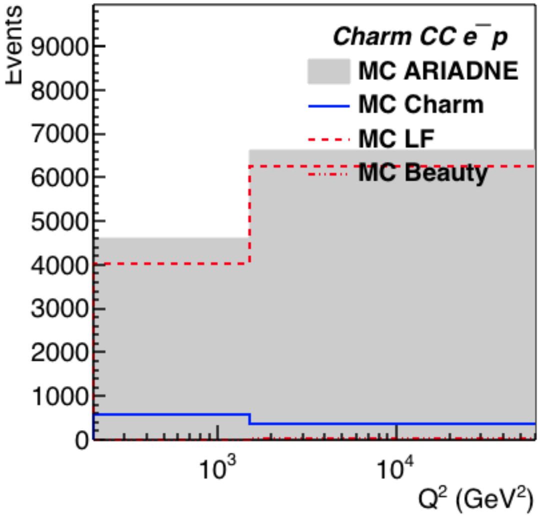

N_{gen}

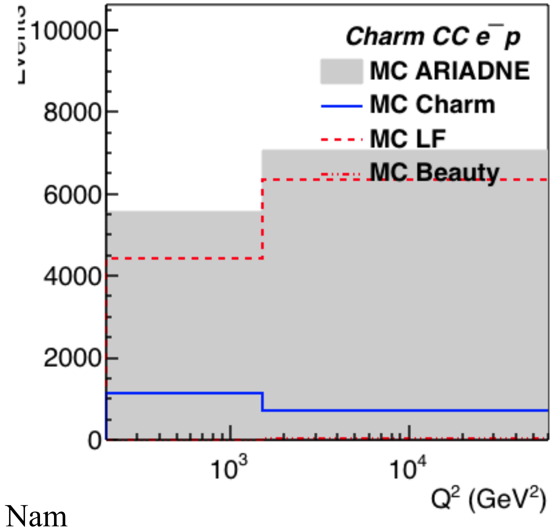

Charm signal & Charm generated

Year	Bin	N_{kin}^{EW}	N_{kin}	N_{gen}^{EW}	N_{kin}^{EW}/N_{kin}	$C_{ext,i}$	C_{ext}
0304p	1	101	105	230	0.96	2.28	
	2	55	60	129	0.92	2.34	
	1+2	156	165	359	0.94	2.30	
	Full space			468			3.00
05e	1	390	412	772	0.95	1.98	
	2	202	260	419	0.78	2.07	
	1+2	592	672	1190	0.88	2.01	
	Full space			1563			2.64
06e	1	149	158	304	0.95	2.03	
	2	77	100	166	0.77	2.16	
	1+2	226	258	470	0.88	2.08	
	Full space			619			2.74
0607p	1	396	414	819	0.96	2.07	
	2	220	240	463	0.91	2.11	
	1+2	615	654	1282	0.94	2.08	
	Full space			1677			2.72

- Full space: $Q^2 < 200\ GeV^2$ && $> 60000\ GeV^2$
- $C_{ext,i} = N_{gen,i}^{EW}/N_{kin,i}^{EW}$ where i runs over for bin 1, 2 and 1+2.
- $C_{ext} = N_{gen,full}^{EW}/N_{kin,1+2}^{EW}$

- N_{gen} = # of events generated in the MC.
- N_{kin} = # of jets associated with charm quark by $\sqrt{\Delta\phi^2 + \Delta\eta^2} < 1$.
  - $\Delta q = q^{jet} - q^{charm}$
  - At the moment, Mc_jet variables are used. Suggestions?
- Visible total charm cross section:

$$\sigma_{c,vis} = \frac{M^{DATA} - M_{bg}^{MC}}{M_c^{MC}} \frac{N_{c,kin}^{MC}}{L}$$

- Visible EW charm cross section:

$$\boldsymbol{\sigma_{c^{EW},vis} = \sigma_{c,vis} - \sigma_{c^{QCD},vis}}$$

$$\boldsymbol{= \sigma_{c,vis} - \frac{N_{c^{QCD},kin}^{MC}}{L}}$$

- Absolute EW charm cross section:

$$\sigma_{c^{EW}} = \frac{N_{c^{EW},gen}^{MC}}{N_{c^{EW},kin}^{MC}} \sigma_{c^{EW},vis}$$

Systematic Uncertainties

Sources	Variable	Variation	$\delta\sigma^{+}_{cEW}$	$\delta\sigma^{-}_{cEW}$
DIS selection			Negligible	Negligible
Secondary Vertex selection	N^{trk}_{secvtx}	> 1	**Statistics limited**	**Statistics limited**
Calorimeter	E_T	$\pm 3\%$	Negligible	Negligible
LF background	N_{LF}	$\pm 30\%$	Negligible	Negligible
QCD charm fraction	$\frac{N_{QCD}}{N_{charm}}$	$+100\%$	$-0.57\,pb$	$-1.1\,pb$
		-100%	$+0.62\,pb$	$+1.7\,pb$
Rescaling			$-1.6\,pb$	$+1.5\,pb$
Signal Extraction	S_{thresh}	± 1	**Statistics limited**	**Statistics limited**
Total			$+0.6\,pb$	$+2.3\,pb$
			$-1.7pb$	$-1.1\,pb$

δ_1 DIS Selection & **Secondary vertex selection**

- Uncertainty associated with the selection threshold values.

δ_2 Calorimeter

- Due to imperfect calibration of hadronic calorimeter (HAC). Uncertainty in E_T^{jet} is known to be ±3%.

δ_3 Background

- Asymmetry in LF decay length due to long-lived LF particles.

δ_4 QCD charm fraction in MC

- Uncertainty associated with the QCD charm fraction calculated in MC is tested by varying the fraction by $\pm 100\%$.

δ_4 Secondary Vertex Rescaling

- More secondary vertices survive in MC than in data. Rescaling was only applied to the light-flavor signal to account for different causes of the discrepancy.

δ_5 **Signal Extraction**

- Due to the low statistics & high fluctuation in data, further study will be performed.

Results

- 0304p & 0607p, 05e & 06e combined at the cross section level.
- Total EW charm cross sections are measured to be

Visible Charm

$$\sigma^{+}_{c,vis} = 4.0 \pm 2.8\ (\text{stat})\ ^{+0.02}_{-0.6}\ (\text{syst})\ pb$$

$$\sigma^{-}_{c,vis} = -3.0 \pm 3.8\ (\text{stat})\ ^{+0.5}_{-0.06}\ (\text{syst})\ pb$$

Visible EW charm

$$\sigma^{+}_{c^{EW},vis} = 3.8 \pm 2.8\ (\text{stat})\ ^{+0.3}_{-0.5}\ (\text{syst})\ pb$$

$$\sigma^{-}_{c^{EW},vis} = -3.6 \pm 3.8\ (\text{stat})\ ^{+0.8}_{-0.5}\ (\text{syst})\ pb$$

EW charm

$$\sigma^{+}_{c^{EW}} = 11.0 \pm 7.7\ (\text{stat})\ ^{+0.6}_{-1.7}\ (\text{syst})\ pb$$

$$\sigma^{-}_{c^{EW}} = -9.6 \pm 10.0\ (\text{stat})\ ^{+2.3}_{-1.1}\ (\text{syst})\ pb$$

- FFN scheme (dashed, blue):
  - ABMP16.3 NLO pdf set, OPENQCDRAD
- FONLL scheme (dashdotted, blue):
  - NNPDF31 NLO pdf set, APFEL
- ZMVFNS (hatched, green)
  - HERAPDF2.0 $f_s = \frac{s}{d+s}$ varied from 0.3 to 0.5.

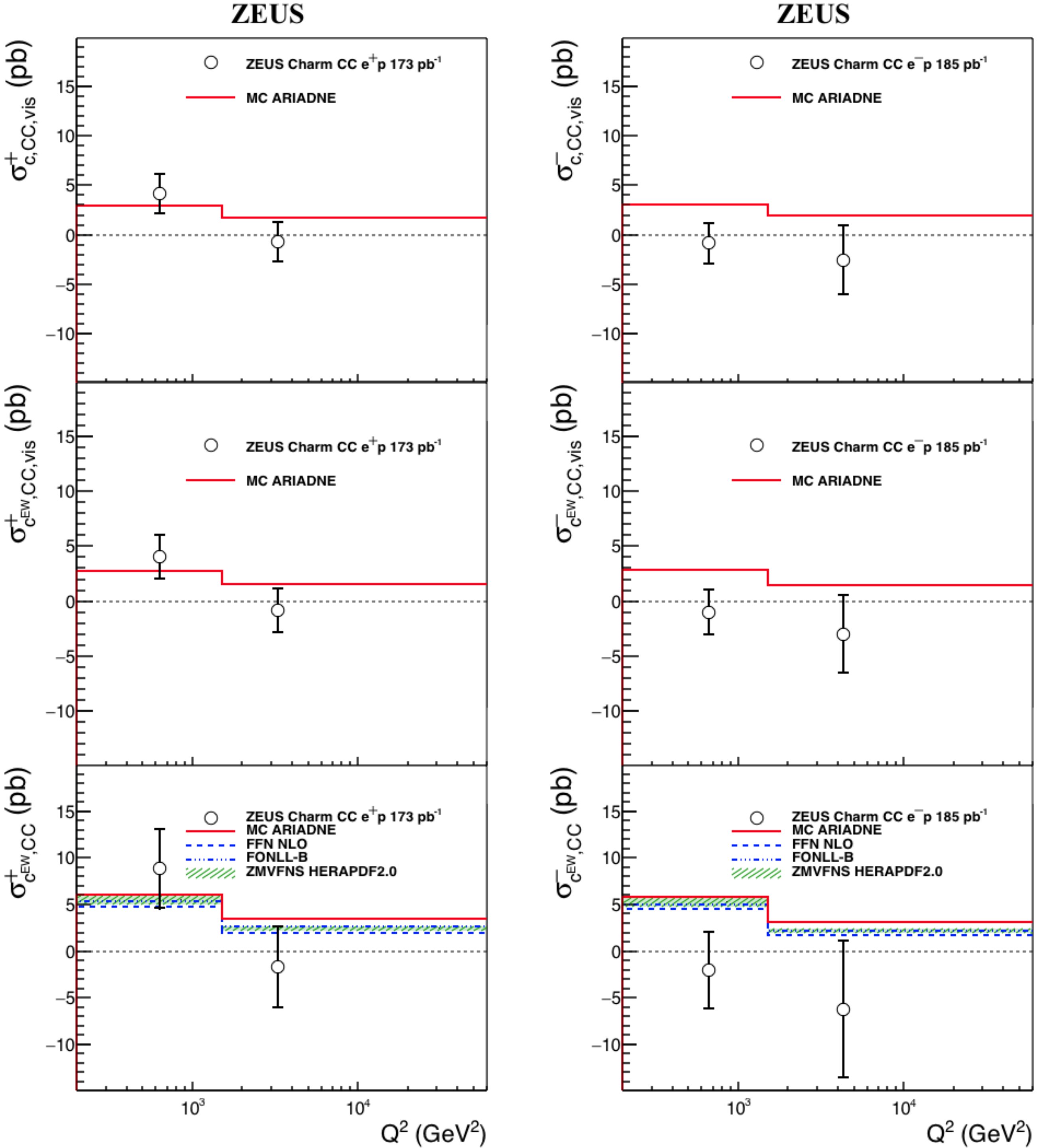

Results

- ZMVFNS with ATLAS-epWZ16 included (dotted line).

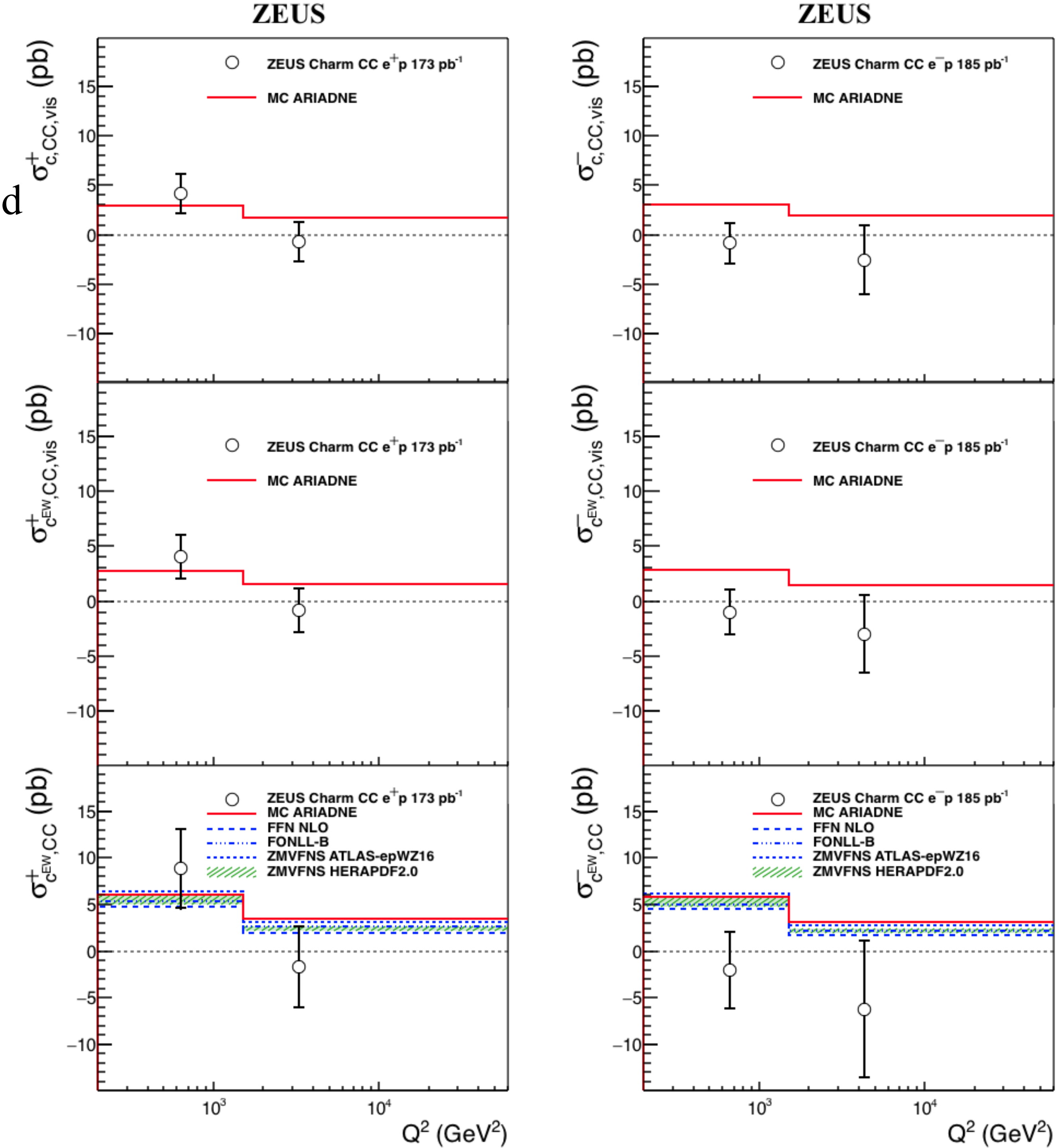

Theory predictions & recap of charm subprocesses

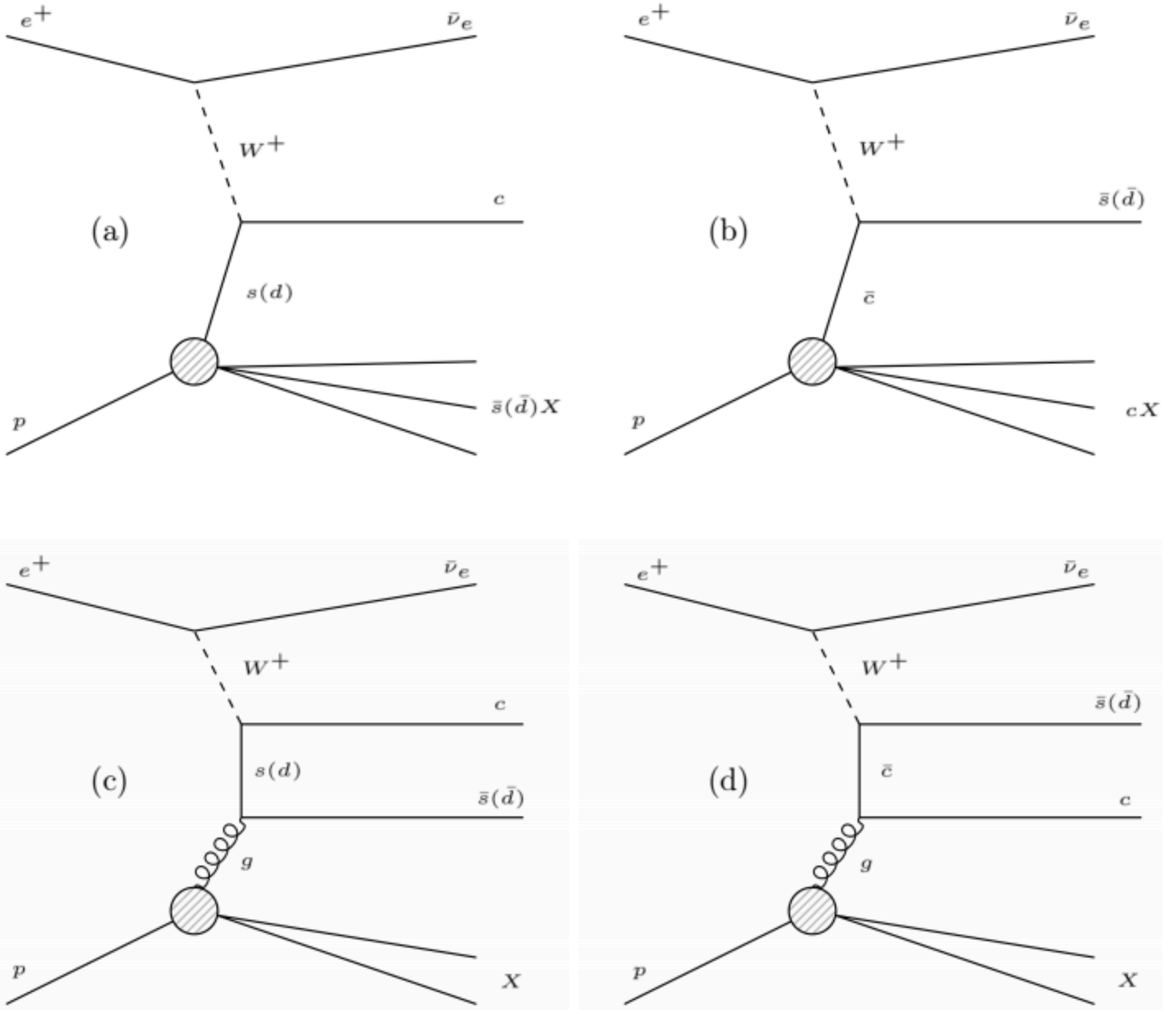

	$d \to c$	$s \to c$	$\bar{c} \to \bar{s}(\bar{d})$
MC	(a) + (c)	(a) + (c)	(b) + (d)
FFN	(a) + (c)	(a) + (c)	(d) w/ larger gluon content
FONLL	(a) + (c)	(a) + (c)	(b) + (d)

e^+p	Contribution (%)					
	$200 < Q^2 < 1500\,\text{GeV}^2$			$1500 < Q^2 < 60000\,\text{GeV}^2$		
	$d \to c$	$s \to c$	$c \to s(d)$	$d \to c$	$s \to c$	$\bar{c} \to \bar{s}(\bar{d})$
MC	6	36	58	10	26	64
FFN NLO	8	49	43	16	43	41
FONLL-B	8	43	50	12	37	51

e^-p	Contribution (%)					
	$200 < Q^2 < 1500\,\text{GeV}^2$			$1500 < Q^2 < 60000\,\text{GeV}^2$		
	$\bar{d} \to \bar{c}$	$\bar{s} \to \bar{c}$	$c \to s/d$	$\bar{d} \to \bar{c}$	$\bar{s} \to \bar{c}$	$c \to s/d$
MC	3	37	60	2	29	69
FFN NLO	4	51	45	5	49	46
FONLL-B	4	43	54	4	33	63

Breakdown of charm subprocesses

Absolute

Year	Bin	$s \to c$	$d \to c$	$\bar{c} \to \bar{s}$	$\bar{c} \to \bar{d}$
0304p	1	0.35	0.06	0.55	0.03
0304p	2	0.26	0.09	0.61	0.03
0304p	1 + 2	0.32	0.07	0.57	0.03
05e	1	0.37	0.03	0.57	0.03
05e	2	0.29	0.02	0.66	0.03
05e	1 + 2	0.34	0.02	0.60	0.03
06e	1	0.37	0.03	0.57	0.03
06e	2	0.28	0.02	0.66	0.04
06e	1 + 2	0.34	0.03	0.60	0.03
0607p	1	0.36	0.06	0.55	0.03
0607p	2	0.26	0.10	0.61	0.03
0607p	1 + 2	0.32	0.08	0.57	0.03

Visible

Year	Bin	$s \to c$	$d \to c$	$\bar{c} \to \bar{s}$	$\bar{c} \to \bar{d}$
0304p	1	0.50	0.07	0.41	0.02
0304p	2	0.43	0.14	0.41	0.02
0304p	1 + 2	0.48	0.09	0.41	0.02
05e	1	0.52	0.04	0.42	0.02
05e	2	0.48	0.04	0.45	0.03
05e	1 + 2	0.51	0.04	0.43	0.02
06e	1	0.52	0.04	0.42	0.02
06e	2	0.48	0.04	0.45	0.03
06e	1 + 2	0.51	0.04	0.43	0.02
0607p	1	0.50	0.07	0.40	0.02
0607p	2	0.43	0.14	0.41	0.02
0607p	1 + 2	0.48	0.10	0.41	0.02

- The QPM like process dominates charm production in the visible region (~60%) as compared to in the full region (~40%) according to MC.

Theory predictions

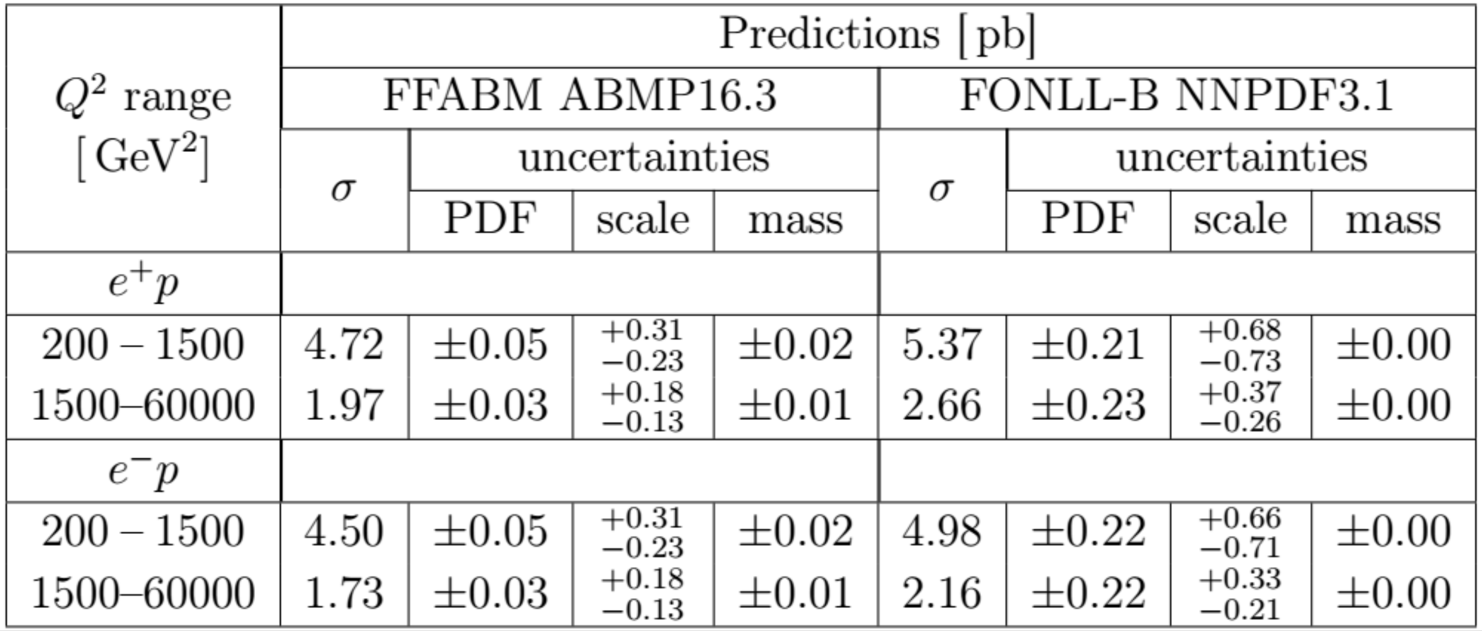

Q^2 range [GeV^2]	Predictions [pb]							
	FFABM ABMP16.3				FONLL-B NNPDF3.1			
	σ	uncertainties			σ	uncertainties		
		PDF	scale	mass		PDF	scale	mass
e^+p								
200 – 1500	4.72	±0.05	$^{+0.31}_{-0.23}$	±0.02	5.37	±0.21	$^{+0.68}_{-0.73}$	±0.00
1500–60000	1.97	±0.03	$^{+0.18}_{-0.13}$	±0.01	2.66	±0.23	$^{+0.37}_{-0.26}$	±0.00
e^-p								
200 – 1500	4.50	±0.05	$^{+0.31}_{-0.23}$	±0.02	4.98	±0.22	$^{+0.66}_{-0.71}$	±0.00
1500–60000	1.73	±0.03	$^{+0.18}_{-0.13}$	±0.01	2.16	±0.22	$^{+0.33}_{-0.21}$	±0.00

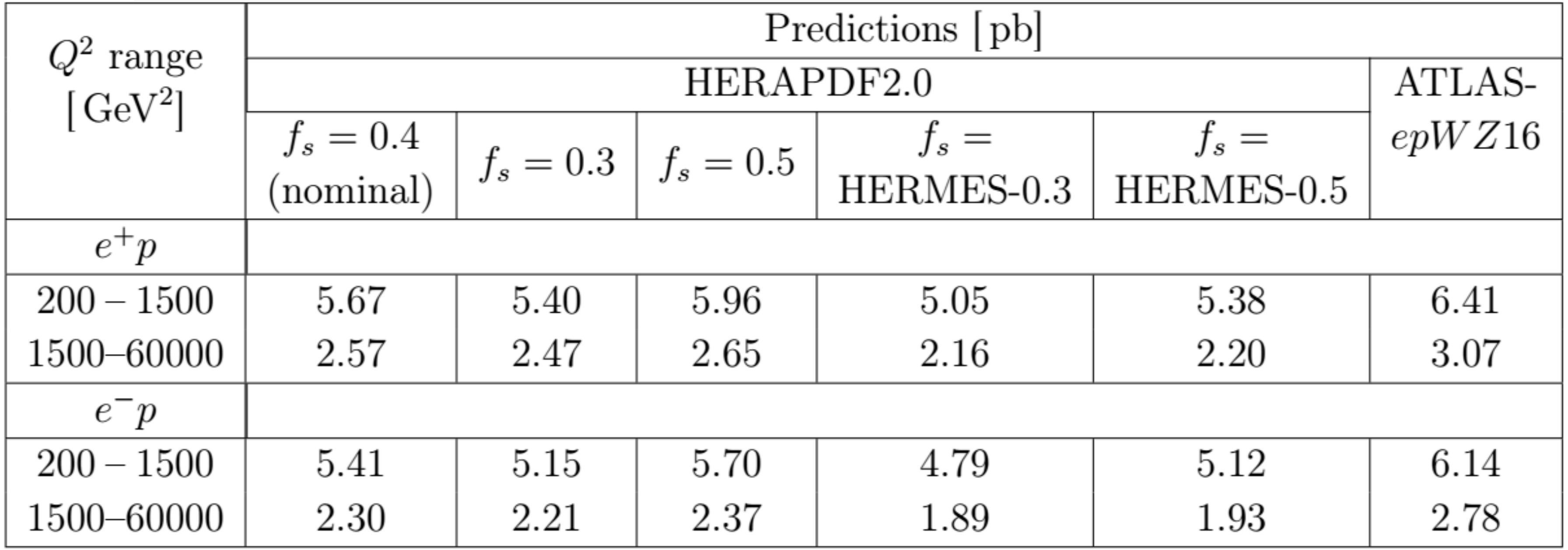

Q^2 range [GeV^2]	Predictions [pb]					
	HERAPDF2.0					ATLAS-$epWZ16$
	$f_s = 0.4$ (nominal)	$f_s = 0.3$	$f_s = 0.5$	$f_s =$ HERMES-0.3	$f_s =$ HERMES-0.5	
e^+p						
200 – 1500	5.67	5.40	5.96	5.05	5.38	6.41
1500–60000	2.57	2.47	2.65	2.16	2.20	3.07
e^-p						
200 – 1500	5.41	5.15	5.70	4.79	5.12	6.14
1500–60000	2.30	2.21	2.37	1.89	1.93	2.78

Summary

- Measurements on EW Charm production in CCDIS has been performed; separately for $e^{+}p$ and $e^{-}p$.
  - EW charm production has been measured within a kinematic region $200 < Q^2 < 60000\ GeV^2, y < 0.9,\ E_T^{jet} > 5\ GeV\ and\ -2.5 < \eta^{jet} < 2.0$
  - Two major contributors are the QPM process $s \rightarrow c$ and BGF process $g \rightarrow c\bar{s}$ sharing about equal contribution.
    - Larger QPM process contribution in the visible region.
  - New definition for visible cross sections.
  - Systematic uncertainties with secondary vertex selection & signal extraction are not considered.
  - New theory predictions have been included in the final plots (Thanks to Sasha!).

Back Up

Determination of η^{jet} upper cut

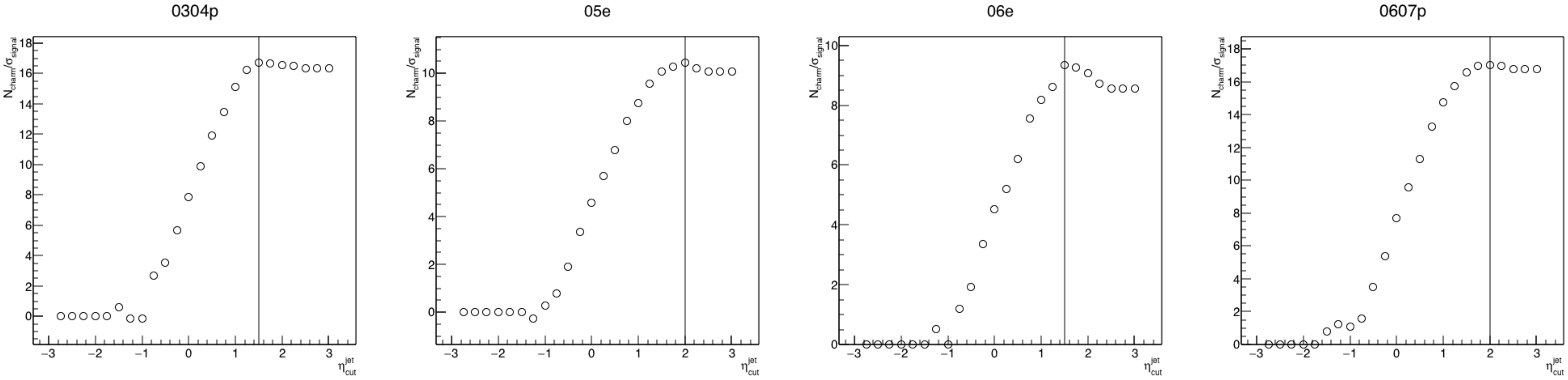

- $\frac{N_{charm}^{MC,mir}}{\sigma_{signal}^{MC,mir}}$ projected from MC as functions of η_{cut}^{jet} per different run period.
  - Highlighted in red vertical lines are the cut locations that would yield the highest ratio.

- In this presentation, $\eta^{jet} < 1.5$ for 05e (STT coverage), $\eta^{jet} < 2.0$ for else.
  - If not placed on the optimal position, the new η^{jet} cut will not reduce statistical uncertainty significantly.

Secondary Vertex Scaling

(0607p)

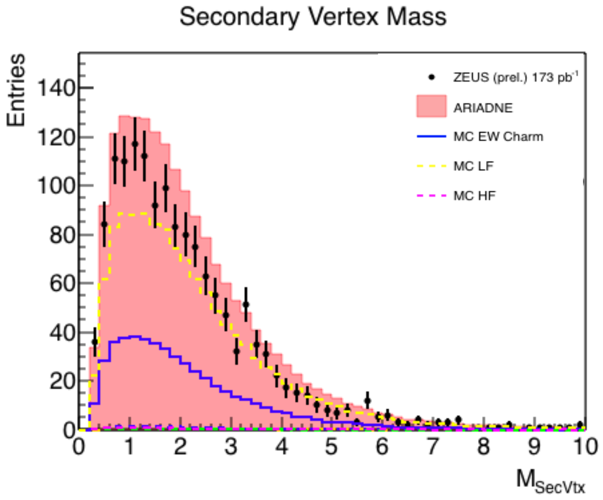
Secondary Vertex Mass

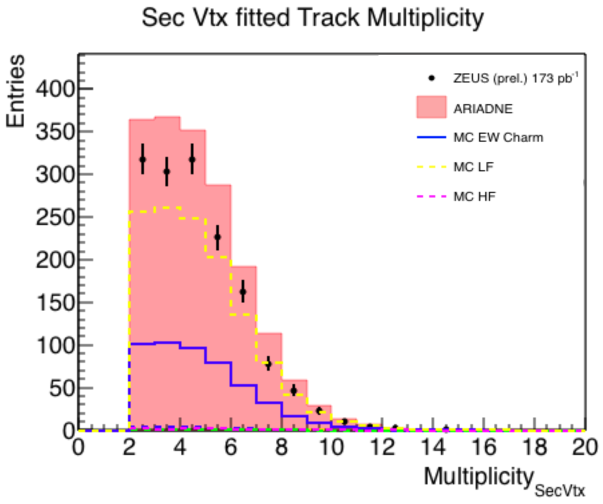
Sec Vtx fitted Track Multiplicity

MC scaling factor = 0.830

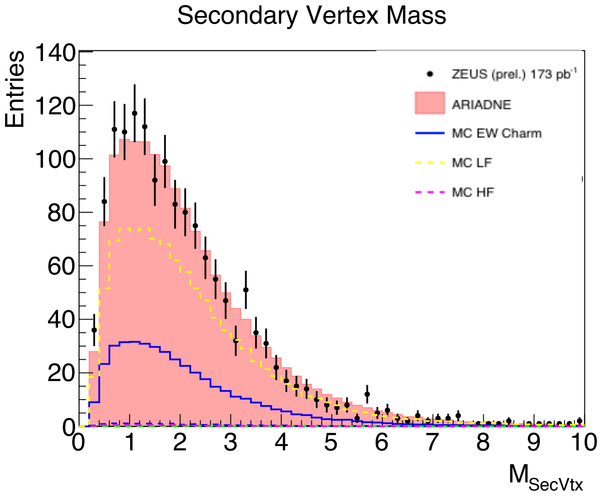
Secondary Vertex Mass

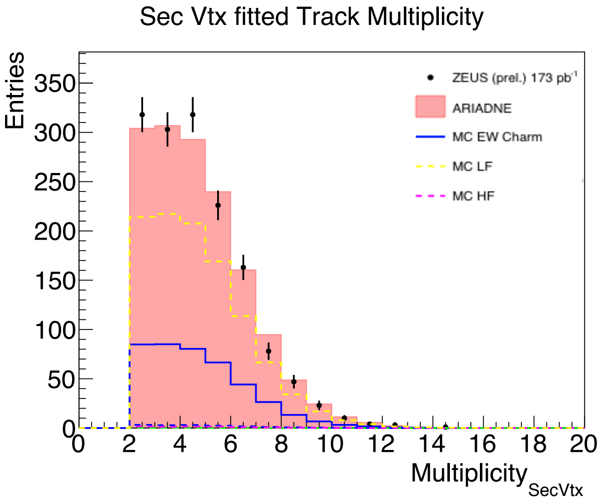
Sec Vtx fitted Track Multiplicity

- MC overestimates trackings & secondary vertices.
- A secondary scaling applied to MC to match Data.

$$\begin{aligned} N^{DATA}_{SecVtx}/N^{MC}_{SecVtx} &= 0.708\ \ (0304p) \\ &= 0.810\ \ (05e) \\ &= 0.807\ \ (06e) \\ &= 0.830\ \ (0607p) \end{aligned}$$

Determination of N_{secvtx}^{trk} cut

0304p

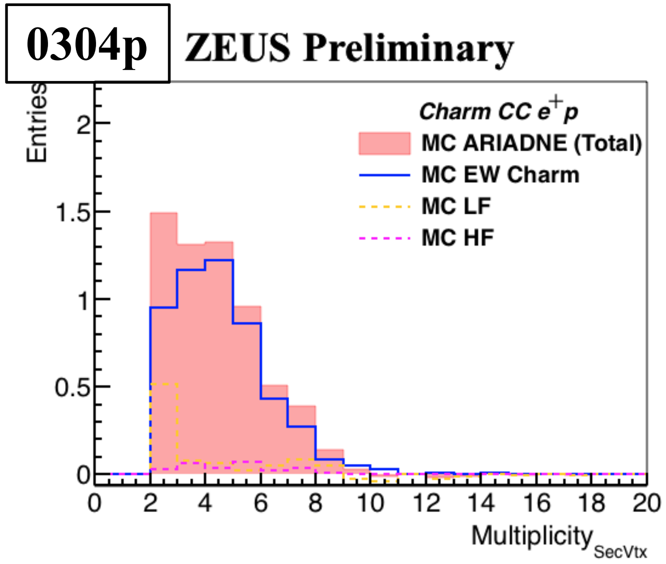

0607p

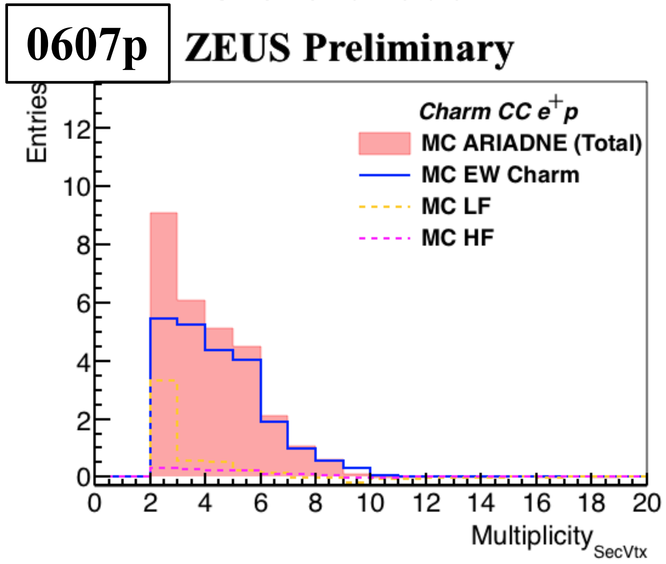

05e

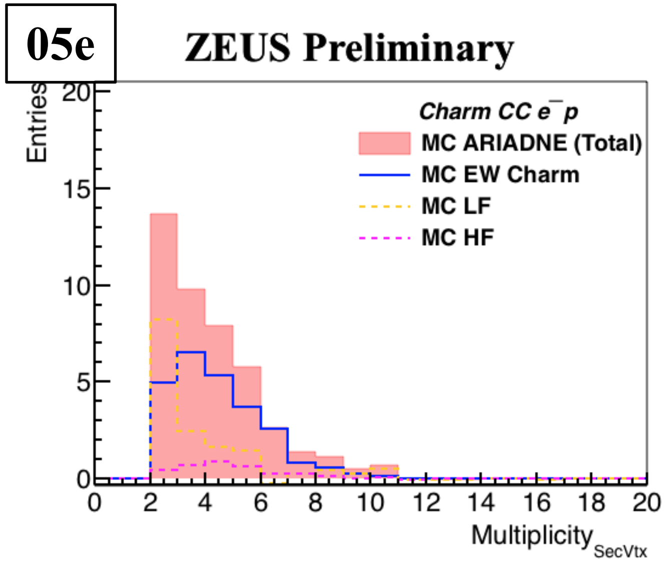

06e

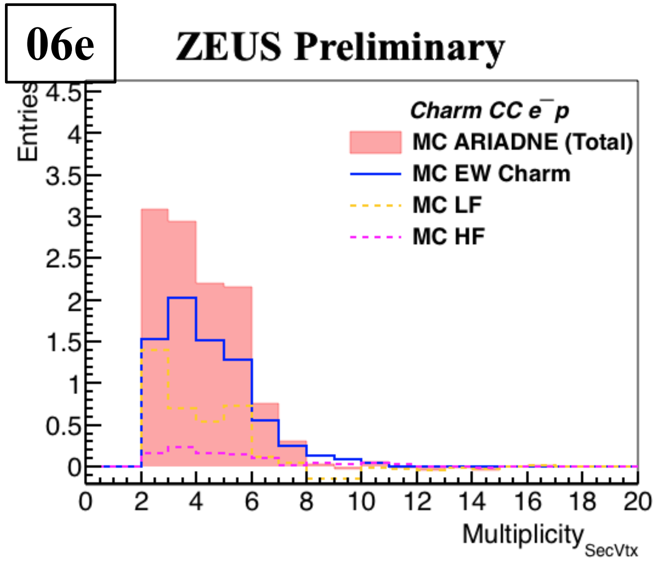

- A high concentration of LF background in low N_{secvtx}^{trk} region is observed across all run periods.

- A LF rejection cut was applied at $N_{secvtx}^{trk} > 2$.

Determination of Significance Threshold

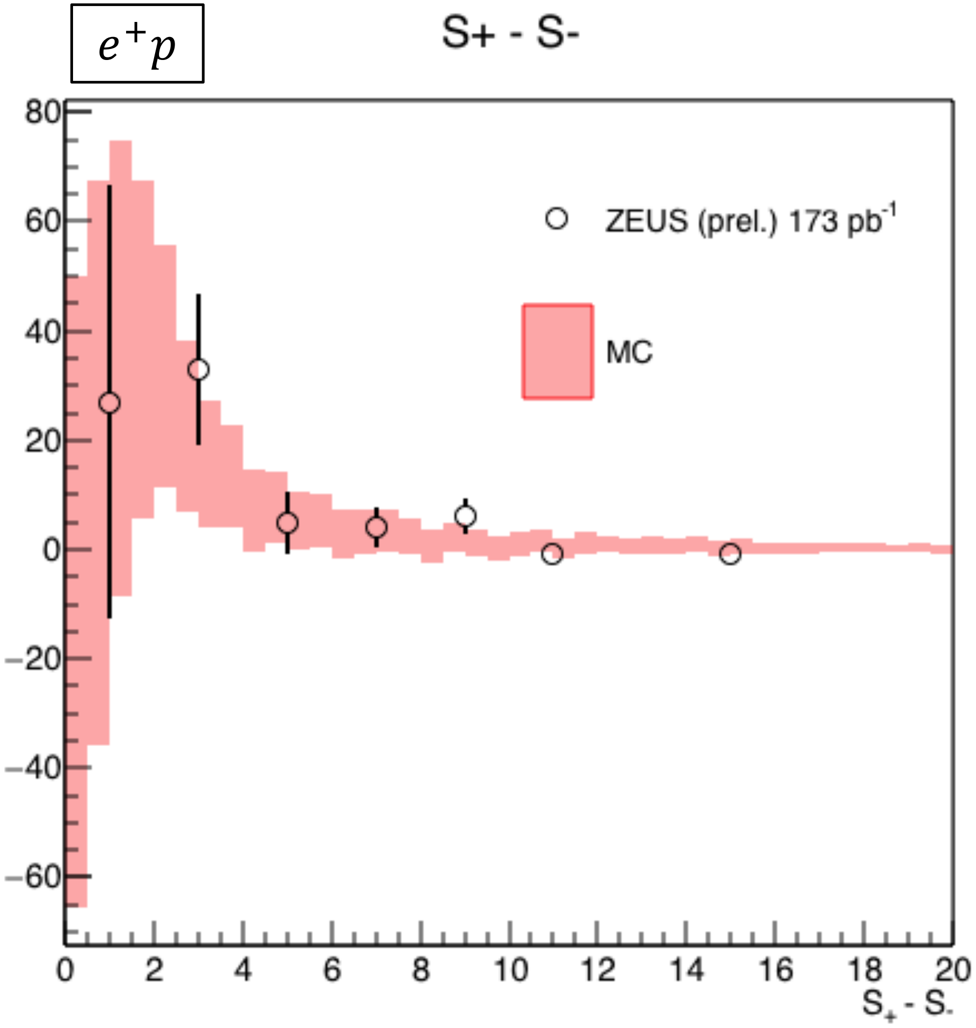

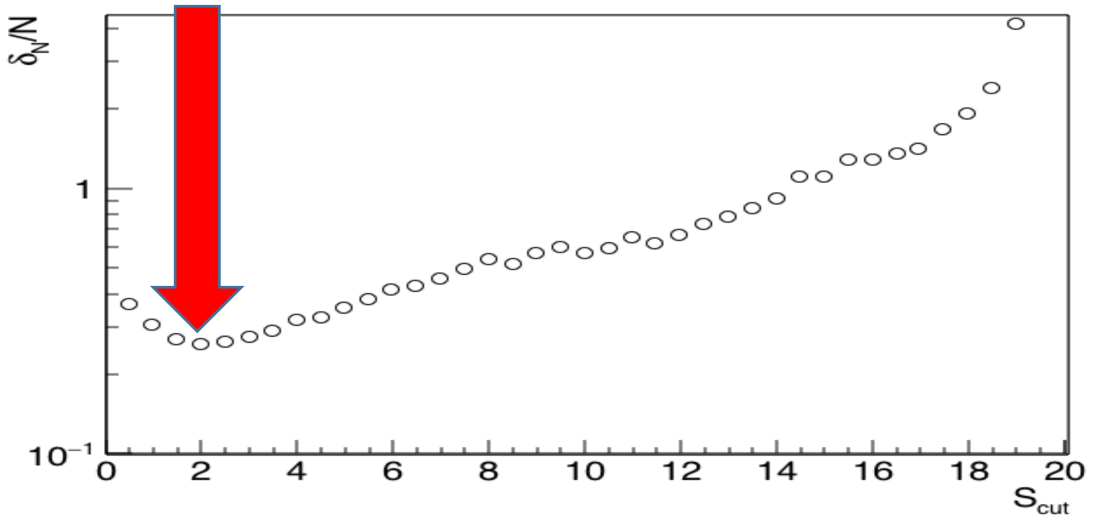

- The high symmetry and large statistics around $S{\sim}0$ contributes to a large statistical uncertainty.
- A significance threshold cut was applied to reduce overall statistical uncertainty.
- From MC, the lowest δ/N is achieved if cut were to be applied at $S = 2$.

Systematic uncertainties (secvtx multiplicity)

e^+p

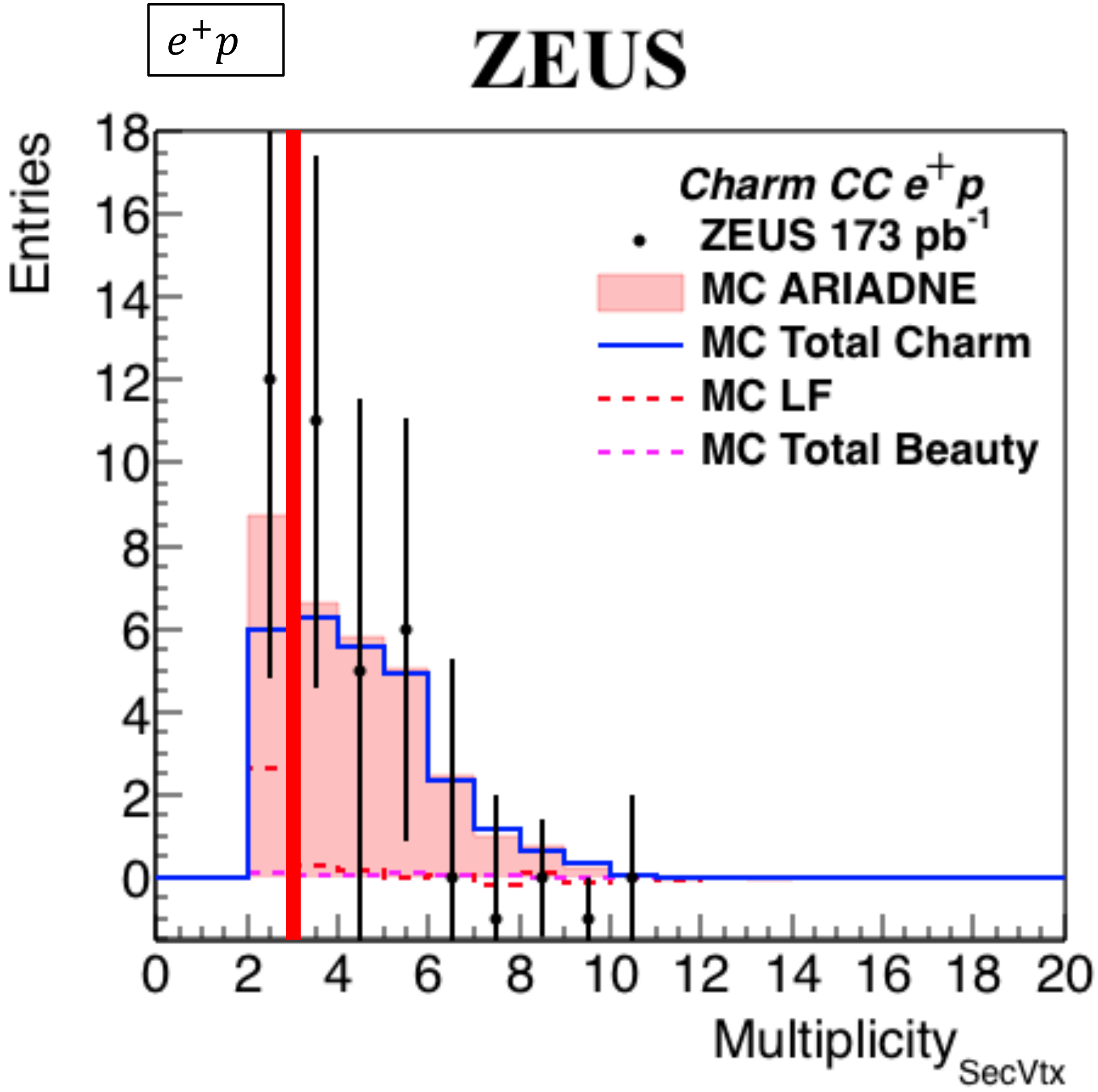

e^-p

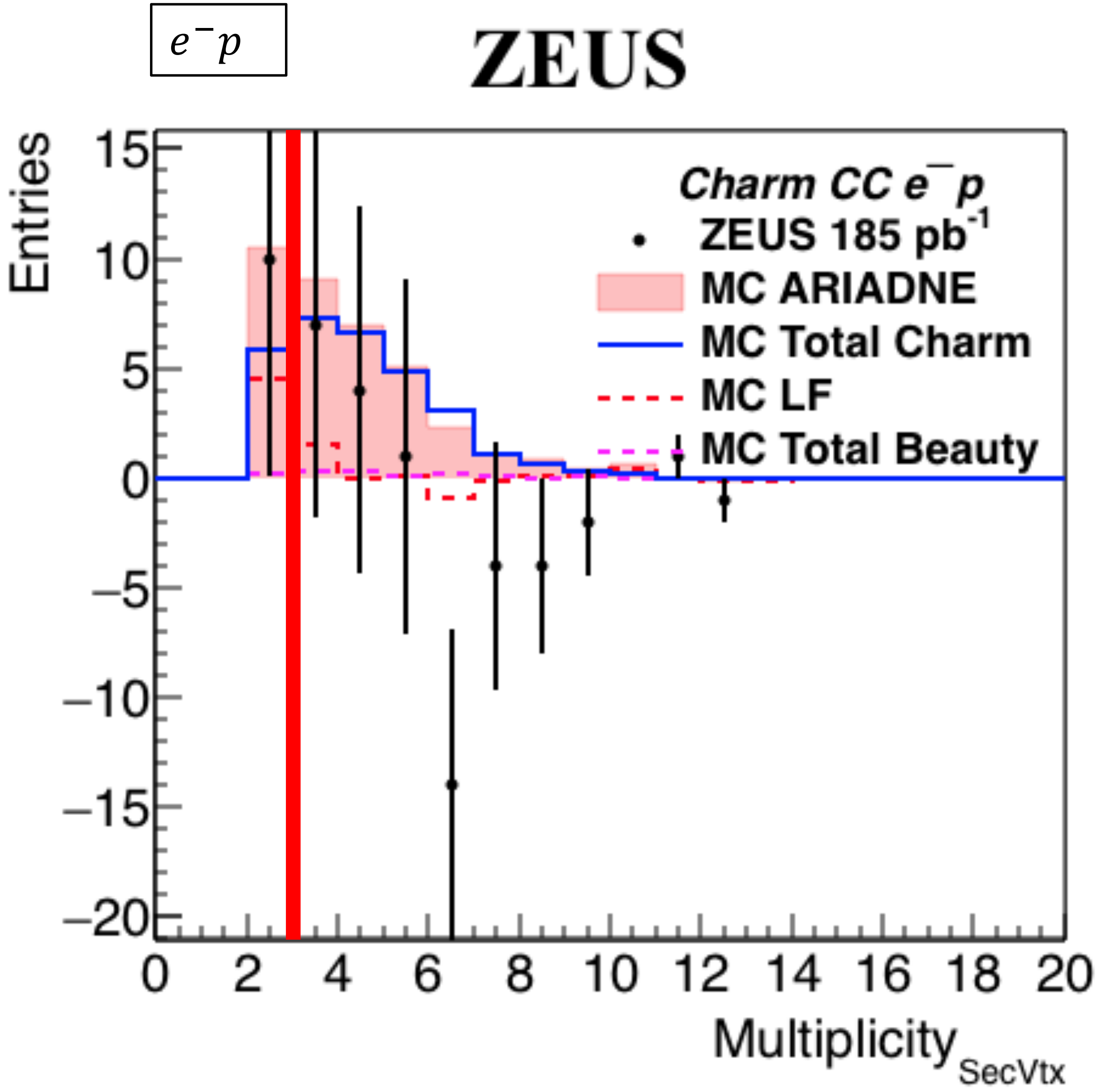

Mirrored significance distribution

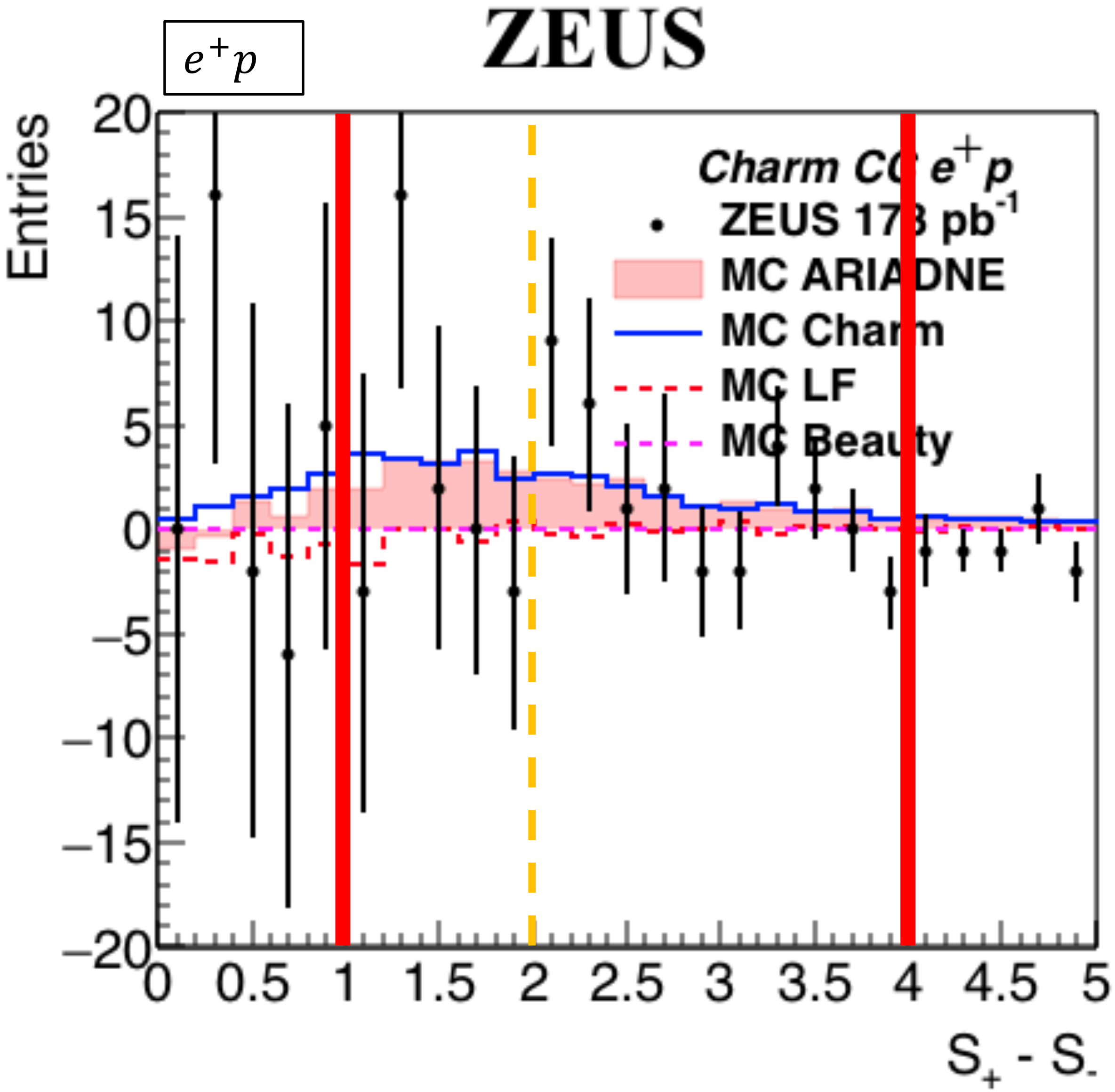

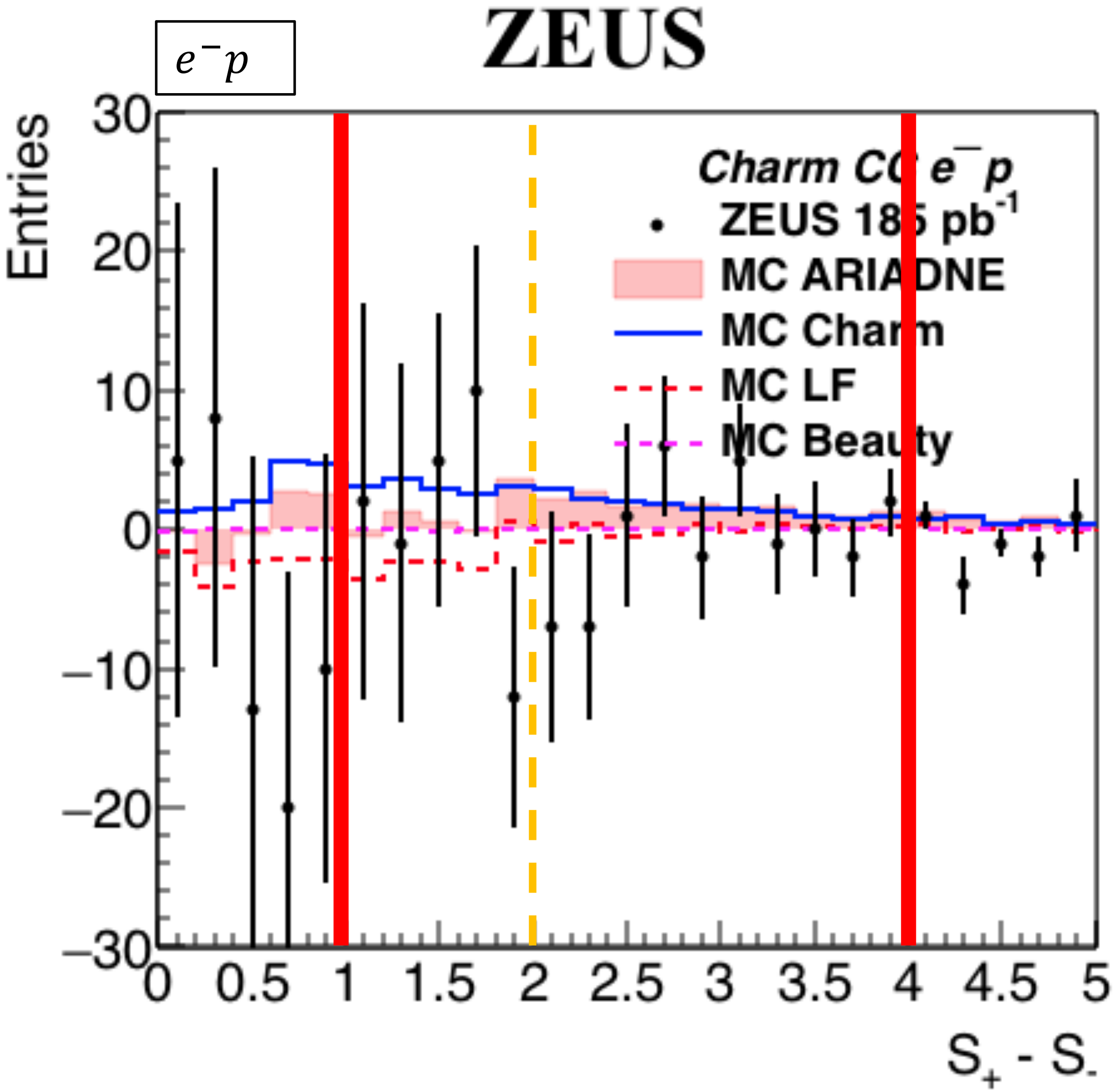

Systematic uncertainty (signal extraction)

Bin 1

Bin 2

Bin 1 + 2

$\sigma_{c^{EW},vis}$
$(e^{+}p)$

$\sigma_{c^{EW},vis}$
$(e^{-}p)$

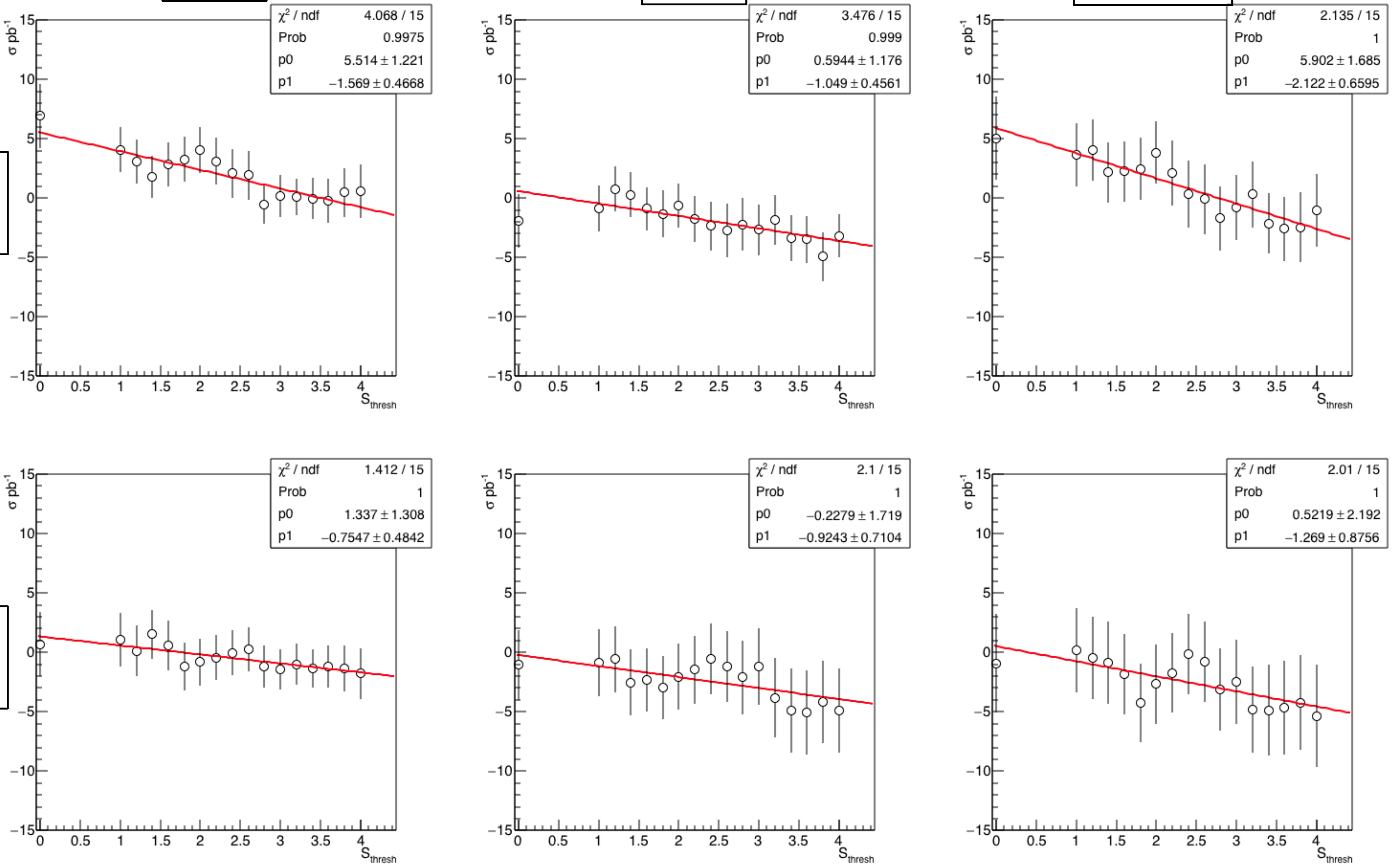

Systematic uncertainties (signal extraction)

$Bin\ 1$ $Bin\ 2$ $Total$

$\sigma^{e^+p}(S_{thresh})$

$\sigma^{e^-p}(S_{thresh})$

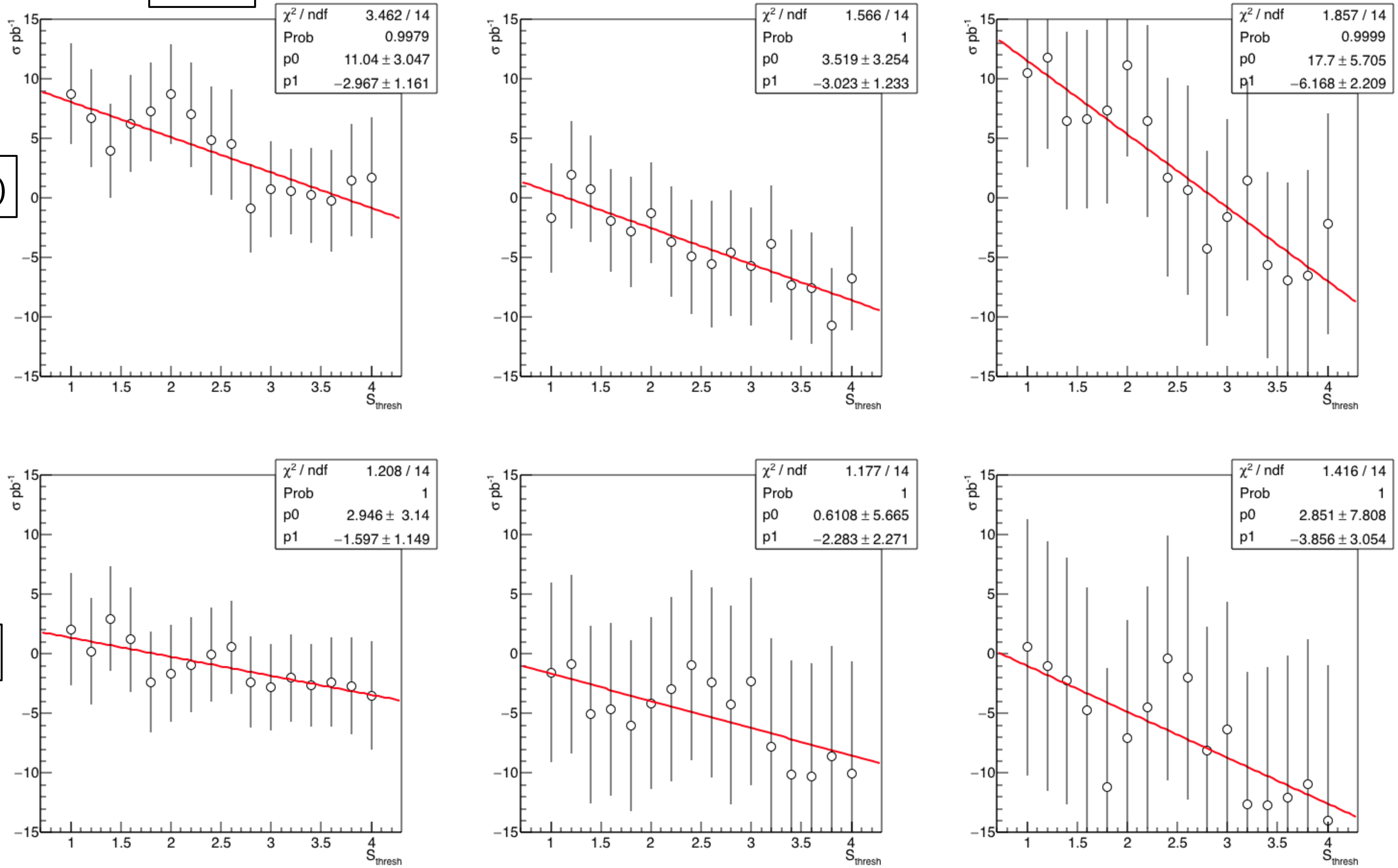

Reconstructed variables

- Good agreement between True and Reconstructed Q^2

$$N_i = \sum_j C_{ij} M_j$$

$N_i = true\ number\ of\ entries\ in\ bin\ i$
$M_i = reconstructed\ number\ of\ entries\ in\ bin\ i$
$C_{ij} = correlation\ matrix\ element\ for\ bin\ i,j$

Collision	C_{11}	C_{22}
e^+p	0.99	1.01
e^-p	0.98	1.02

e^+p

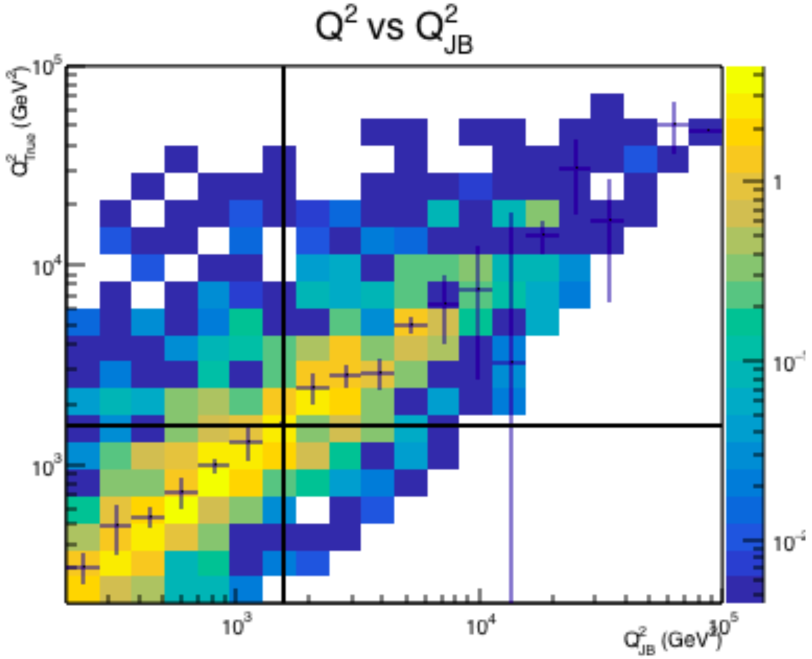

Q^2 vs Q^2_{JB}

e^-p

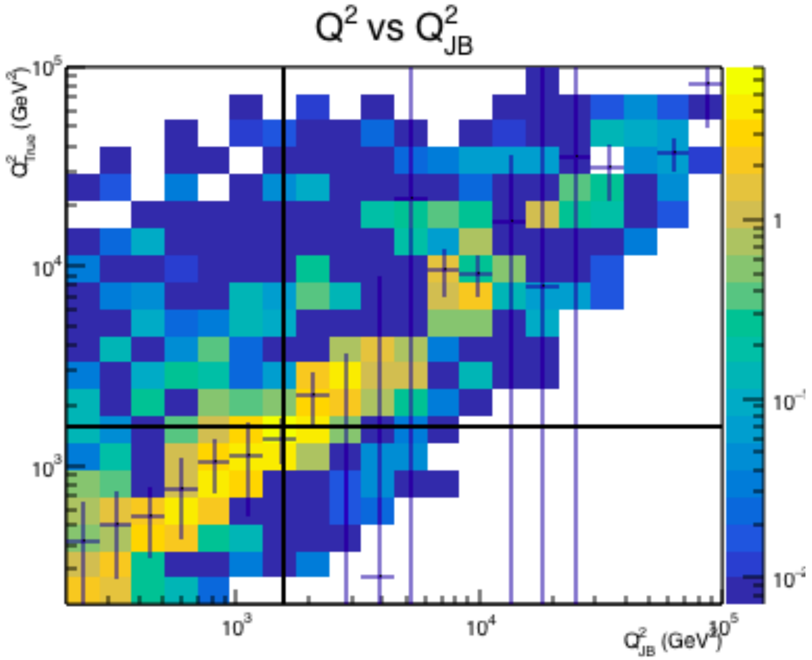

Q^2 vs Q^2_{JB}